An Approach for Optimization of Features using Gorilla Troop Optimizer for Classification of Melanoma

Anupama Damarla*, Dr Sumathi D
SCOPE, VIT-AP University, Vijayawada, Andhra Pradesh, India

***Abstract*—The diagnosis and categorization of skin cancer, as well as the difference in skin textures and injuries, is a tough undertaking. Manually detecting skin lesions from dermoscopy images seems to be a difficult and cumbersome challenge. Recent advancements in the internet of things (IoT) and artificial intelligence for clinical applications have shown significant increase in precision and processing time. A lot of attention is given to deep learning models because they are effective at identifying cancer cells. The diagnosis and accuracy levels can be greatly increased by categorizing benign and malignant dermoscopy images. This work suggests an automated classification system based on a deep convolutional neural network (DCNN) in order to precisely perform multi-classification. The DCNN's structure was thoughtfully created by arranging a number of layers that are in charge of uniquely extracting different features from skin lesions. In this paper, we proposed a deep learning approach to tackle the three main tasks-deep extraction of features (task1) using transfer learning, selection of features (task2)-using metaheuristic algorithms such as Particle Swarm Optimization (PSO), Ant Colony Optimization (ACO), and Gorilla Troop Optimization (GTO) as a feature selector, the extensive feature set is optimized, and the amount of features is reduced to within the range, and a two-level classification (task3) was proposed that are emerging in the field of skin lesion image processing. On the HAM10000 dataset, the proposed deep learning frameworks were assessed. The accuracy achieved on the dataset is 93.58 percent. The proposed method outperforms state-of-the-art (SOTA) techniques in terms of accuracy. The suggested technique is however highly scalable.**

Keywords—*Skin cancer; image enhancement; deep learning; evolutionary algorithms; Particle Swarm Optimization; Ant Colony Optimization; Gorilla Troop Optimization*

I. Introduction

Epidermis cancer is an invasive disease produced by aberrant melanocyte cell development on the body that tends to reproduce and propagate through lymph nodes, destroying healthy tissue [1]. The ozone layer, that provides protection against UV rays [2] which is depleting causes an increase in skin cancer. On the skin's surface, damaged cells create a lesion that can either be benign or malignant. Melanoma is considered the deadliest form of skin cancer worldwide which emerged as a common disease with highest mortality [3]. Also, it is classified as cancer since it is more hazardous and life-threatening. Melanoma starts in the melanocyte cells, which seem to be brown or black in color and mimic a lesion [4]. Approximately 2500 females and 4700 males have expired due to melanoma in 2019 [5]. Males have a higher likelihood of developing melanoma than females, according to statistics shown in Fig. 1 [6]. However, precise, reliable early detection is very important as discovered lesions have a 90.0 per cent survival rate [7].

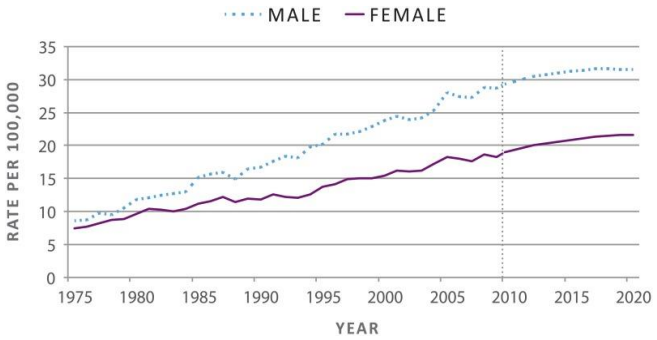

Fig. 1. Age- Adjusted Melanoma Incidence Rates from 1975-2020 [6].

II. Related Work

Although the various table text styles are provided. The formatter will need to create these components, incorporating the applicable criteria that follow.

Skin cancer detection is challenging due to the diversity in skin textures and injuries. Dermatologists therefore employ dermoscopy, a non-invasive tool, to identify skin irregularities at an initial level [8]. The foremost move in dermoscopy was applying the gel for the diseased region. After that, a magnifying tool is used to obtain a magnified image. This magnified image allows you to see the structure of the lesion region more clearly. The dermatologist's experience determines the accuracy of the detection [9]. According to a survey, the detection precision of a dermatologist might range from 75 per cent to 84 per cent [10]. Contrarily, manual dermoscopy diagnosis requires a lot of time and has a significant chance of error, including for dermatology with experience [11]. As a result, studies developed a number of computer-aided diagnostic (CAD) systems using deep CNN features [12].

The acquisition of a three primary stages of a CAD system is a skin imaging dataset, feature extraction and selection, and classification [13]. Data on skin cancer are unreliable and conventional methods are parameterized and require standard normal training data. Each lesion has a unique pattern and therefore these treatments are ineffective. Dermatologists can

*Corresponding Author.

accurately identify malignancies with the help of deep learning methods for classifying skin. In comparison to classic feature extraction strategies, the use of epidermis lesion with deep features identification and classification has become increasingly important in recent years [14]. Deep characteristics, which were used to categorize data, are generated from the completely connected layers of a CNN model. Unlike traditional methods like hue, texture and contour, deep features encompass both local and global information about a picture. The convolutional layer extracts local information such as edge, pixel which differs immediately with adjacent pixels of an image; whereas the 1D layers (global average pooling and fully connected) gather global information such as shape descriptors, contour representations [15]. In traditional techniques, geometric information such as Histogram of Gradients, color and textures (Local Binary Patterns) are extracted independently [16].

Even though deep learning algorithms are extremely adept at processing complicated data, skin categorization remains a difficult task for several reasons:

1) As demonstrated in Fig. 2, the distribution of skin lesion classes in the current dataset is unbalanced, with more than 60% of the photos belonging to the NV: "Melanocytic nevus" class and some classes being extremely rare (less than 2%). The lesion images are classified into seven categories as shown in Table I, with number of lesions.

2) Hairlines, water bubbles, ruler marks, etc. are all examples of noisy artefacts in lesions shown in Fig. 3.

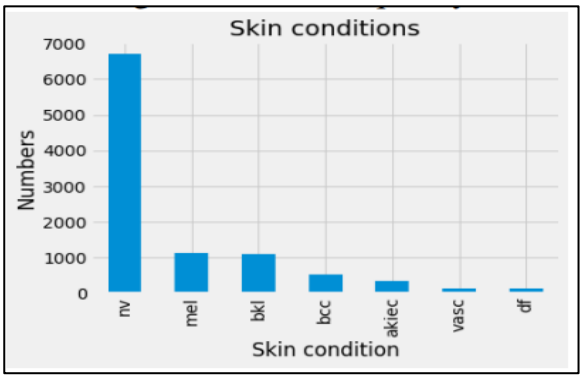

Fig. 2. Class Imbalance [52].

TABLE I. SKIN LESIONS AND INSTANCES COUNT IN HAM10K DATASET [38]

Skin Type	Instances Count
Actinic Keratosis (Akc)	326
Basal Cell Carcinoma (Bcc)	514
Dermatofibroma (Df)	116
Melanoma (Ml)	1114
Nevus (Nv)	6704
Pigmented Benign Keratosis (Bkl)	1098
Vascular Lesions (Vsc)	143
Total	10015

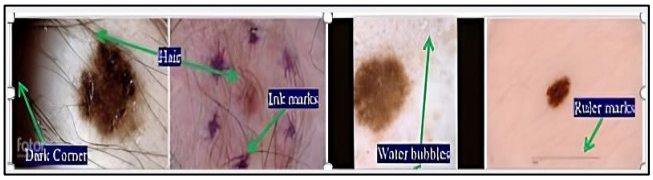

Fig. 3. A Typical Pictorial Presentation of the Skin Images in ISIC 2017 Test Dataset [17].

3) Lacerations are hard to differentiate due to significant intra class variances and inter class commonalities in terms on color, size, site and appearance.

Furthermore, there have been a few obstacles in the development of classification systems and they are provided as given below:

- Initially, there is a discrepancy in the data and there aren't many images with labels.
- Lesser complicated & lighter network designs.
- When techniques are used to categorize skin cancers that are uncommon in the training sample, a misdiagnosis is frequently the outcome.
- Millions of pixel high-resolution images frequently require extensive computing and extra training.
- The different circumstances will cause different noises to be produced (such as different imaging devices, backgrounds).

While prominent pre-trained deep learning networks are trained on diverse datasets, such as ImageNet, they are not used for skin cancer concerns in general [53]. A method for picking the best subset of features based on shape and color to build better and final categorization is required. As a result, the proposed approach shown in Fig. 4 intends to create, implements, and estimate a highly efficient deep learning-based system for malignant vs. benign categorization.

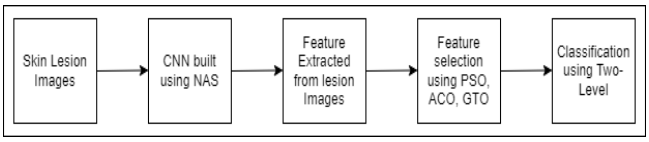

Fig. 4. Flow Structure of Whole Network.

The following is a breakdown of the remaining sections: Section II discusses the research on Neural Architecture Search and optimizers. A public dataset is used in proposed work for skin cancer detection is presented in Section III. In Section IV, a proposed method that explains the CNN, feature selection with three optimization approaches for efficiency with classification in detailed is explained. The results and discussions implemented on the dataset as well as outcomes analysis with other optimizers are seen in Section V, and finally, in Section VI, conclusions are formed.

III. LITERATURE SURVEY

Several methodologies and procedures have been developed for categorization of skin lesions [8]. Zafar et al [18] proposed two pre-trained CNNs U-Net and ResNet called

Res-Unet for segmenting lesion boundaries and significantly improve the classification accuracy. Computer vision-based machine learning approaches were used in the developed methodologies. Machine-learning algorithms made use of supervised learning and deep learning techniques for the accurate identification, segmentation, and classification of epidermis tumors [19]. Aziz et al. [20] used deep features from a pre-trained AlexNet network, which were then classified using SVM. Their method yielded good results in terms of lesion categorization. Ren et al. [21] presented a fusion mechanism [22]. J. Zhang et al. [23] suggested a CNN for epidermis categorization that consisted of several attentions residual learning (ARL) units succeeded by global average pooling and classification layers. Yu et al. [24] developed a CNN-based design that was pre-trained on several picture resolutions. It developed a fully convolutional residual network (CRN) for segmentation and deep residual network (DRN) for classification. Majtner et al. [25] used a used local binary pattern features and hand-crafted Rsurf features for melanoma recognition system. Ahonen et al [26] uses LBP texture features for efficient facial recognition. A new method to analyze the data which were then segmented zone wise and classified using a Support Vector Machine (SVM) [27] algorithm is proposed. On the HAM10000 dataset, Sivasai et al. [32] proposed a DCNN for lesion classification based on MobileNetV2 and Long Short-Term Memory (LSTM). MobileNetV2 outperformed existing CNN models in several ways, which include reduced computational cost, tinier network size, and interoperability with smart devices. Wannipa et al [43] presented a light weight deep CNN called MobileNet for classification of skin lesions. Ahmed et al [44] presented an ensemble CNN model that combines ResNet 50 and InceptionV3 architectures to classify the seven different skin lesion types. The below Table II provides the comparative analysis.

Prior to the attention in deep learning, research on neural architecture search had been undertaken. Three factors characterize each NAS framework: search space, search strategy and performance evaluation technique [28]. NAS was created to find and develop the model that perfectly suits the dataset in use. As a result, the NAS model has a minimal set of parameters but good performance. Models suited for both small and large datasets can be found using NAS [30]. The Global search space and the Cell search space are two types of search spaces. The network-based technique investigates the entire system, whereas the cell-based approach identifies only the cells, which were subsequently stacked to address a task [29]. The count of cells in the stack is determined by the work at hand. Melanoma detection and classification using dermoscopic images, researchers used a deep learning [31] approach. Deep feature extraction was done with a deep residual network, and image encoding was done. To detect and categorize melanoma using discriminating dermoscopy images, SVM classification with chi-square was used. On the difficult ISBI 2016 dataset, the provided technique performed admirably.

Feature selection (FS) is gaining popularity which is a technique for minimizing the dimensionality of data. It reduces data intricacy by deleting superfluous contents that is critical. This method minimizes the model's complex nature by including only the most relevant features, making it easier to interpret. By filtering out redundant data, FS approaches reduce the dimensionality of network data. As a consequence, FS is a crucial component of data preparation in medical analysis since it impacts accuracy results. Any feature selection problem could be roughly described as an optimization problem. Several Feature selection methods elicited from metaheuristics (MH) methodologies were recently been implemented. Numerous search techniques mainly inspired by nature and mimicking principles of biology, physics, ethology, or swarm intelligence, have been effectively included in metaheuristic algorithms [34]. Those were split into two categories: standard solution-based approaches and population-based approaches. Population-based algorithms have better ability than single solution-based algorithms [35]. The population-based algorithms are categorized into multiple categories: (1) Particle Swarm Intelligence algorithms (SIs), (2) Evolutionary Algorithms (EAs), (3) Natural Phenomenon algorithms (NP). Grasshopper Optimization Algorithm (GOA), Whale Optimization Algorithm (WOA), Elephant Herding Optimization (EHO), Harris Hawks Optimization (HHO), and Moth-flame Optimization (MFO) are some well-known metaheuristic algorithms [36]. The study indicates that population-based algorithms are well suited to solving real-world problems, despite the need for more objective functions [37].

TABLE II. SUMMARY OF LITERATURE REVIEW

Paper ID	Dataset	Model	Accu %	Limitations
[18]	ISIC 2017, PH2	Res-Unet	77.2, 85.4	Need augmentation to prevent overfitting
[19]	ISIC 2017, ISIC 2016	ResNet50, ResNet101	80.6, 91.8, 89.1, 86.8	Dilated convolution, Group Normalization
[20]	-	AlexNet, ResNet18	93.3, 93.8	-
[21]	ISIC 2017	DenseApp	76.9	Model is complex
[22]	ISIC 2017, PH2	MB-DCNN	80.4, 89.4	Improve task Performance simultaneously
[23]	ISIC 2017	ARL-CNN50, ResNet50	91.8, 90.5	Unsupervised Attention learning
[24]	ISBI 2016	FCRN	85.5	Prob graphical models
[25]	-	Rsurf, LBP	80.2	-
[32]	HAM10K	MobileNetV2, LSTM	85	Feature extraction based on biomarkers
[43]	HAM10K	MobileNet	-	-
[44]	-	ResNet-IncepV3	89.9	-

TABLE III. DATASET, METHODS, ACCURACIES AND CLASSES FOR SKIN CANCER

Author	Model	Accuracy %	Classes
Achim et al(2019)	CNN with XGBoost	82.95	5
Pratik et al(2019)	CNN	82	7
Duyen et al(2020)	ResNet50	93	7
Deif et al(2020)	InceptionV3	89.81	2
Shahin et al(2021)	DCNN	91.93	2
Hatice et al(2022)	Insinet	94	2
Mahbubur et al(2022)	DiffusionFiltering	91.65	2

The procedures outlined above follow certain automated lesion classification techniques. The Deep learning models have higher feature extraction accuracy than pre-trained models, and then applying nature-inspired metaheuristic algorithms as a new feature selection model, a latest method for binary-to-multi classification based on deep learning are the top-performing steps. The aim of maximization of accuracy degree of any subset is shown in Table III. The large number of features produces biased findings since data patterns of training set are not uniquely identifiable in testing data. The drawbacks of metaheuristic techniques get struck with the local optima rather than the global optima.

A. Research Gap

Earlier works have been focused on various features such as shape, texture and color either by fusion or through many other techniques. Hence, the focus of this work is on performing the detection of asymmetric borders along with contrast enhancement. Therefore, this motivated us to do this work.

B. Motivation

- The deep neural network has witnessed growth to the next generation by introducing the concept of optimized network. This idea was materialized through the concept of NasNet.
- The predominant factor is to determine a model that would be robust and intractable to seize the global solutions in this complex problem.
- Color channeling embedded with dimension has been given more attention.
- Combining these techniques will achieve high performance.

The solution strategy that does not meet the same efficiency to solve all the problems motivated to propose this method.

IV. METHODOLOGY

The proposed method for skin cancer detection, which is provided in this part, used deep learning and nature inspired algorithms as a feature selection models that aims to improve the performance and the efficiency on selected features. Fig. 5 depicts the architecture of the suggested technique. This method has five main layers: Image acquiring and preprocessing; Extraction of features using NasNet Large; optimizing the features using PSO, ACO, and GTO; finally, a Two-level classification.

C. Dataset

The dermoscopic method has improved the accuracy of skin cancer diagnosis. With the help of this invasive skin imaging technique, skin lesions can be captured and the clarity of the spots is improved. In this section, the most used dataset named HAM10000 Dataset is utilized to carry out the experimental process, in this area of research. It was investigated in the HAM10000 dataset that samples belonging to minor classes can be detected by popular CNN models.

HAM10000 Dataset: The HAM10k "Human Against Machine with 10,000 Training Images" collection is most famous publicly accessible dataset, containing 10k raw dermoscopic images primarily utilized to detect pigmented epidermis Laceration. Fig. 6 depicts several types of skin cancer. Due to the low inter-class and significant intra-class variance difficulties as shown in Fig. 7 the classification of these skin types is difficult.

The dataset was split into three sections: training, validation, and test. The training set received 70 per cent of the total samples, the validation set received 10 per cent, and the test set received the remaining 20 per cent as shown in Table IV. To provide the network enough training, the percentage of samples within the train set was maintained at a higher level. The network's performance was tracked using validation data to fine-tune the settings. Finally, the network's performance was assessed using the test data.

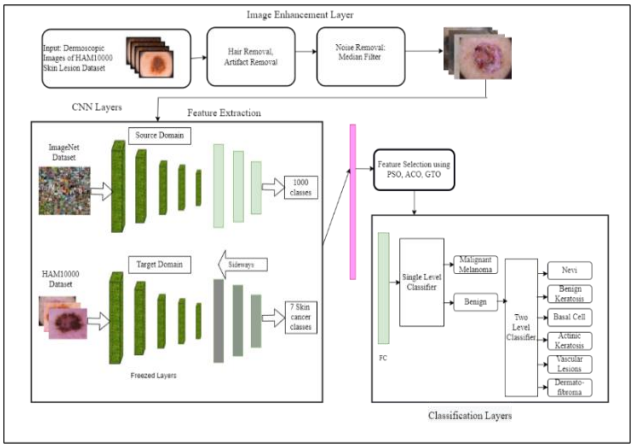

Fig. 5. Skin Lesion Classification using Two-Level Classifiers.

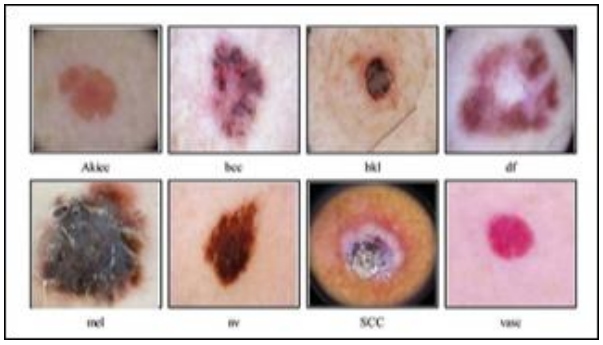

Fig. 6. Sample Skin Lesion types of HAM10000 Dataset [33].

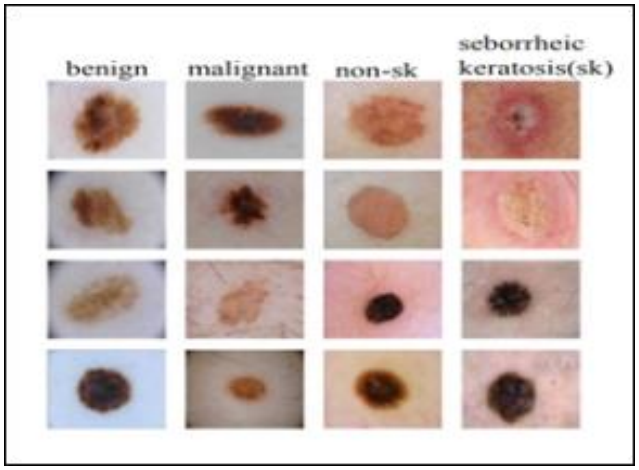

Fig. 7. Skin Lesion Images with Low Inter-class and Significant Large Intra-class Variance [54].

TABLE IV. THE HAM10000 DATASET PROPORTIONS AMONG TRAIN, VALIDATION, AND TEST [39]

Category	Train Samples	Validation Samples	Test Samples	Total Samples
Malignant	3181	454	909	4544
Benign	3830	547	1094	5471
Total	7011	1001	2003	10015

D. Image Enhancement

During the acquisition, coding, transmission, and processing of digital images, noise is constantly present. Noise in an image is defined as an abrupt change in pixel values. Removing noise from digital images is exceedingly difficult without prior knowledge of filtering processes. Image data filtering is a standard step in almost all image processing systems. Filters are used to accomplish this. They reduce noise from the image while retaining their characteristics. The type of data and the filter's behavior determine which filters are used. Various preprocessing filtering techniques, such as mean, median, wiener, and nonlocal means filters, are used to enhance the acquired images.

The initial step in any type of medical image processing is to perform enhancement that aims to improve the quality of the original images and make the subsequent stages of operations easier. Reflections, hair follicles, epidermis lines, air bubbles, and shadows are all common artefacts in skin photographs that affect the image segmentation stage. Intensity correction, color space transformation, artefact removal, and contrast adjustment are some of the approaches that have been introduced for image enhancement. The median filter shown in (1) is a simple way to improve the quality of photographs by eliminating artefacts.

$$y\,[m,n] \;=\; median\,(x\,[i,j],(i,j)\;\in\;w) \qquad (1)$$

where w describes the weight of neighbors and [m,n] is the median point in the image.

Median filtering is a nonlinear method for image smoothing as shown in Fig. 9. This filter can be used to smooth skin lesion photos and remove artefacts while maintaining the lesion boundaries. The median filter mask size should really be proportional to the main image to achieve operative smoothing. The pattern of neighbors is used as the 2D window which slides pixel by pixel over the image. They extend border values outside with values at boundary. The median of all image pixels within the window will be used to replace the central pixel. The filter's principal operation is arranging all the pixel values from the window into ascending order and replacing the considered pixel with the middle pixel value. (If the neighborhood has an even pixel count, the average of two middle pixel values is used.) The pseudocode is given below:

```
for (p1=0; p1<n; p1++)
    for (p2=0; p2<n; p2++)
        if(I[p1] < I[p2])
        {       w=I[p1]
                I[p1] = I[p2]
                I[p2] = w
        }
```

Moreover, the filter that has been adopted in this work may be used to smooth pictures, softening large frequency distortions like as noise, additional lines, and hair while preserving crucial information like type, texture, configuration, color and location about the lesions. In contrast to linear filters, which maintains the original image with no edge blurring? Fig. 9 depicts the results.

E. NasNet Large Features Extraction

With the help of the challenging image database ImageNet [37], a deep Neural Architecture Search (NAS) [36] model has been implemented on more than a millions of images. The NasNet Large requires images with an input size of 150 by 150. The Recurrent Neural Network (RNN) in NAS generates a child network with a distinct structure. The holdout method is used to train the child networks to ensure accurateness. To improve the network's architecture, the controller is updated by combining the accuracy of the child connections. Fig 8 depicts the controller structure. The controller delivers hyper parameters as tokens for forecasting feed-forward neural networks with convolutional layers. When the layer exceeds a certain value i.e. 6 normal cells, the architecture generation process is paused. Each prediction is made by a Softmax classifier, and the outcome is fed into the next phase. During the models fine-tuning procedure, it initially discards the models the last three layers and adds a new layer depending on the count of dataset classes. Transfer learning is applied to refine the model after the fine-tuning phase. Several key parameters were selected during the training process, such as the learning rate of 0.001, epochs of 20, minimum batch size of 64, and SGD for learning. Following the fine-tuning of a network on epidermis datasets, features from the average pool layer were collected and used for subsequent process, including feature selection.

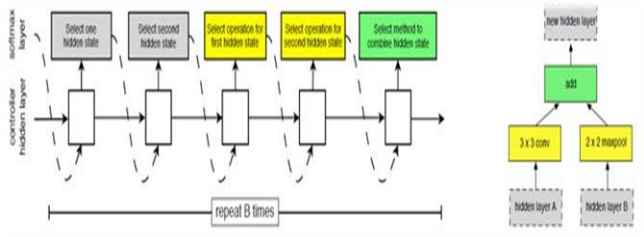

Fig. 8. Controller Architecture Model [45].

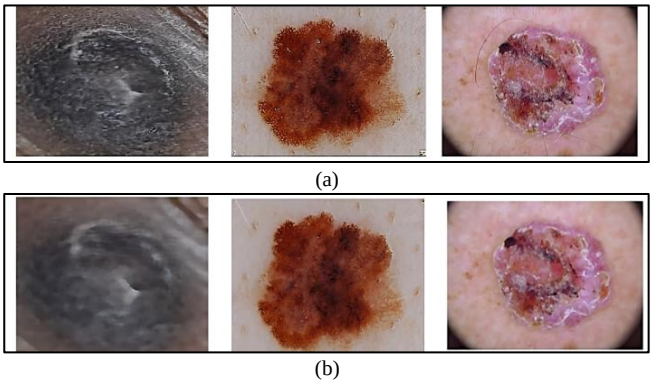

(a)

(b)

Fig. 9. (a) Original Dermoscopic Images, (b) Images after Pre-processing.

F. Feature Extraction using Color Space

As it is known that melanoma is typically brown, black, or tan in color, although it can also be red or pink as shown in Fig. 10. The feature extraction method focuses on obtaining information from color space. It is normalized from RGB color space using RGB_r where Red_r, $Green_r$, and $Blue_r$ are normalized color channels translated from RGB color space. The value of intensities in each pixel is represented by i and j and the dimension of skin images is stated with MxN. There are now three color channels as shown in (2,3,4):

$$Red_r = Red_r(i,j) \quad (2)$$

$$Green_r = Red_r(i,j) - Green_r(i,j) \quad (3)$$

$$Blue_r = Red_r(i,j) - Blue_r(i,j) \quad (4)$$

Fig. 10. Appearance and Location of Melanoma.

G. Metaheuristic Approaches for Feature Selection

Certain metaheuristic approaches are nature-inspired and are commonly utilized in machine learning for selecting features or optimization. Numerous metaheuristic algorithms are not biologically inspired. Fong et al. [46] selected features from five datasets from the UCI repository using the Correlation based FS, PSO and Accelerated PSO techniques. When compared to all features, Decision Tree, Naive-Bayes, SVM, and ANN classifiers have a 12.7 per cent, 1.93 per cent, 2.11 per cent, and 0.3 per cent difference in classification accuracy when just 64 per cent, 26 per cent, 26 per cent, and 64 per cent of the entire features are used. Seijas et al [47] classified the MNIST handwriting dataset with SVM Classifier using 3 metaheuristic approaches: Binary Fish School Search (BFSS), Advanced Binary Ant Colony Optimization, and Binary Particle Swarm Optimization. BFSS, ABACO, and BPSO achieve 93.36 per cent, 90.15 per cent, and 92.08 per cent classification accuracy using just 41 per cent, 22.4 per cent, and 27 per cent of the overall characteristics, respectively. Yeh and Chan [48] retrieved 277 characteristics from the MIAS database using 70 benign, 55 malignant, and 69 normal mammograms. For feature selection, they used the Genetic Algorithm (GA), ACO, SA and PSO. PSO discovered a classification accuracy of 96.9 per cent using only 189 features. Naeini et al. [49] worked on two datasets of high-resolution satellite images captured by the WorldView-2 sensors. From satellite images, a total of 173 characteristics are extracted. Particle Swarm Optimization (PSO), Genetic Algorithm (GA), Artificial-Bee-Colony (ABC), and Honey-Bee-Mating (HBM) algorithms pick Object Based Features (OBF). Their research has revealed that PSO is an inexpensive method for recognizing various entities such as trees, buildings, and roadways. Ighazran et al [50] evaluated sentiment analysis using a metaheuristic feature selection. In certain studies, multiple metaheuristic algorithms are coupled to create an advanced hybrid approach that may operate significantly better in feature selection. Arora et al [51] combined the Grey-Wolf and Crow search algorithms to create an approach. They used a total of more than 20 standard benchmark unimodal, multimodal, and fixed-dimensional multimodal mathematical functions and 21 datasets to evaluate the results of the novel hybrid approach with ten popular MH techniques for selecting of features.

1) Contributions on this work: The selection of the optimal features is a critical step that improves classification accuracy rate while decreasing computing time. Three metaheuristic algorithms, Particle Swarm Optimization (PSO), Ant Colony Optimization (ACO), and Gorilla Troop Optimizer (GTO), are employed in this work to determine an optimum collection of features. GTO chooses an optimum feature set from among these methods to deliver the best classification accuracy of 93.58 per cent. It was discovered that color features are best for classifying skin lesions stated from section 3.4. Higher accuracy is attained in this work using less than 0.4 per cent of all the characteristics selected by the aforementioned optimizations.

H. Metaheuristic Algorithms

The "curse of dimensionality" refers to the challenge of using a larger collection of features, which can create noise and impede system performance. Reasons for selecting a more limited set of features quicker training, reduced difficulty of the model, and improved model precision, among other criteria like computation time, storage, etc. There are several feature selection techniques like feature ranking, feature

transformation, feature subset selection but the proposed study performs feature optimization and for this, three metaheuristic methods are used in this suggested study. These algorithms are all from the nature-inspired category. PSO, ACO and GTO are all population-based algorithms inspired by nature. To select the best technique, we used metaheuristic techniques from several types of algorithms.

1) Particle Swarm Optimization (PSO): PSO emerges for an optimal outcome iteratively by conducting simultaneous searches on a population of solution candidates known as "particles" whose current particle in the search space reflects a candidate's solution [57]. PSO iteratively seeks the best outcome by travelling every particle in a manner that is a summation of the feature vector together across their individual instantaneous velocity, local best position location, and global best position location. Each particle has a social learning rate as well as an individual best-position learning rate. Every iteration, starting with a random value, the location of each particle is altered. The position of each particle is determined with the own individual best position (PBes) (as determined from the fitness function) as well as the best position of all particles in the population (GBes). Using these data, (5) and (6) are used to modify the particle's position (P) and velocity (V):

$$P\ (t_i\ +1)\ =\ -\ P\ (t_i) +\ V\ (t_i\ +1) \tag{5}$$

where

$$V\ (t_i\ +1)\ = V(t_i)\ +\ a_{i1}.ra_{i1}.(PBes(t_i) - P(t_i))\ +\ a_{i2}.ra_{i2}.(GBes(t_i) - P(t_i)) \tag{6}$$

The random number's values ra_{i1} and ra_{i2} ranges between 0 & 1 and a_{i1}, a_{i2} are the learning rates displayed in tabular column 2. The particle's inertia value determines how much of its previous velocity is added to its current velocity. The initial inertia of the particle is its initial inertia. The change in inertia is provided by the inertia damping rate. PSO can be utilized to choose n_s features out of a maximum of $n_T$features. Once particles are allowed to move in n_T-dimensional space, the features corresponding to the ns lowest components of the instantaneous position can be recognized as extracted features. It should be emphasized that the search space's axes correspond to the features, and that the selection of an axis is determined by the readings of the position vector along that axis.

2) Ant Colony Optimization (ACO): To determine the shortest path from their location to the food supply and the vice versa, ants search using a metaheuristic algorithm called ACO [55] [56]. An ant will leave a trail of a specific chemical pheromone on its way of travel when it leaves its nest in search of food. The strength of the pheromone trail left by an ant's predecessor can also be determined. The term "stigmergy" refers to an indirect communication technique that chooses the quickest route from the nest location to the food location. Each way has a starting pheromone deposit level and pheromone evaporation rate. ACO can be employed to choose a series of vertices from a plot where the contours are adaptively balanced by a property called pheromone strength. This property makes sure that an edge that is traversed more often is given more weight. A sequence is produced by the ant's movement. An ant i will select node j at a node with a probability proportional to the strength of the pheromone along the path i–j as shown in (7):

$$p_{ij==\frac{T_{ij}^{\alpha}}{\Sigma_j T_{ij}^{\alpha}}} \tag{7}$$

where, T_{ij} = pheromone level of a contour i, j and α is a constant known as ant pheromone exponential weight. The pheromone updates with (8)

$$T_{ij} ==\ (1\ -\rho)\ T_{ij}\ +\Delta\ T_{ij} \tag{8}$$

where, ρ = evaporation rate & Δτij = deposition in the edge is illustrated in (9):

$$\Delta\ T_{ij} = \Sigma_k \frac{1}{L_k} \tag{9}$$

Here L_k signifies the value of the kth path that moves along the edges i,j. From a total of n_T features, n_s features are chosen using ACO. Also every features can be thought of as a node in a plot, with initial n_s nodes of the ACO series identifying the selected feature. The final set of features chosen is the one with the lowest cost (error of classification) shown in Fig. 12.

3) Gorilla Troop Optimizer (GTO): The GTO is simple to operate and has a limited number of parameters that must be configured. There are three phases for exploration and two for exploitation. Compared to cutting-edge algorithms, GTO's key benefit is that it quickly discovers the best answer. Gorillas are symbolized as X in this algorithm, while silverbacks were being symbolized as GX.

a) Exploration Phase: The exploration stage is primarily used to conduct a global search of space. In GTO [41], every member can be a solution, and at each step of the optimization process, the best solution can be named the silverback gorilla. The following strategies were employed:

1) Transitioning to an anonymized region which searches the entire sample space.

2) Reducing the search area in order to strike a balance among both exploitation and exploration.

3) Ultimately, growing the GTO's capability to examine the region by moving forward towards a known region.

It is numerically expressed in (10,11,12,13,14,15) as:

$$GX(t_i+1)_1= \begin{cases} (tp - bp) \times r_1 + bp, r < p, \\ (r_2 - C) \times X_r(t) + L_g \times H, r \geq 0.5, \\ X(i) - L_g \times \left(L_g \times \left(X(t) - GX_r(t)\right) + r_3 \times \left(X(t) - GX_r(t)\right)\right), r < 0.5. \end{cases} \tag{10}$$

$$C = F_i \times \left(1 - \frac{t}{Max_t}\right) \tag{11}$$

$$F_i = \cos(2 \times r_4) + 1 \tag{12}$$

$$L_g = C \times l \tag{13}$$

$$H = Z_g \times X(t) \quad (14)$$

$$Z_g = [-C, C] \quad (15)$$

where tp = top position

bp =bottom position of the variable,

X(t) = present position of gorilla

GX_r = Single gorilla group of a particular region

GX (t_i + 1) = the candidate level of gorilla in the t+1 iteration.

p = Migration parameters oscillates [0,1]

r_1, r_2, r_3, r_4, rand, l = random values ranging from [0,1]

X_r= Single candidate gorilla

t_i = Current Iteration

Max_t = Total number of Iterations

L_g = used to calculate silverback gorilla

Z_g = Random number ranging from [-C, C]

The fitness value of each GX solution was determined by the algorithm in the conclusion from the exploration phase, and if GX (t_i) < X(t), the X(t) solution is swapped out for the GX(t_i) solution.

b) Exploitation Phase: Two approaches are employed at this point. First is Continue to track the silverback and second is compete for adult female gorillas. The approaches are chosen based on a comparison between C ((11)) and W. (initial values).

Stage 1: If C ≥ W, the silverback gorilla will choose the below (16,17) for survival.

$$GX(t_i + 1) = L_g \times M \times (X(t) - X_{silverback}) + X(t) \quad (16)$$

$$M = \left(\left| \left(\frac{1}{N}\right) \sum_{i=1}^{N} GX_i(t) \right|^{g} \right)^{(1/g)}, g = 2^l, \quad (17)$$

where, X (t) = gorilla position

$X_{silverback}$ = Silverback gorilla position

GX(t_i) = Candidate solution at iteration t

N = Number of gorillas

Stage 2: If C < W, compute the (18, 19, 20, 21) i.e., competing for female mating.

$$GX(t_i) = X_{silverback} - (X_{silverback} \times Q - X(t) \times Q) \times A \quad (18)$$

$$Where, Q = 2 \times r_5 - 1 \quad (19)$$

$$A = \beta \times E, \quad (20)$$

$$E = \{N_1 rand \geq 0.5\ N_2\ frand < 0.5\} \quad (21)$$

r_5 = random value [0,1]

The amount of variables generated by the GTO algorithm equals the amount of features in the dataset. All variables have a range of [0, 1] with 1 representing that the applicable attribute is a classification selection candidate. The algorithm then computes every gorilla's fitness as shown in (22).

$$Fitness_i = \alpha \times (1 - C_i) + (1 - \alpha) \times \frac{|BX_i|}{D} \quad (22)$$

BX_{ij} = 1 if X_{ij} > 0.50

where X_{ij} is the dimension value for search agent i at dimension j and α falls within the [0,1] range, and Ci stands for the measured accuracy. D is the dimension of the input train dataset. The finest solution will be the one with the lowest fitness value. Following that, the agents will be modified utilizing the GTO algorithm stages. The updating stage was repeated until the terminal state was reached. Finally, the GTO method produces the optimal solution that includes the feature set, which is then utilized as the following step in reducing the testing dataset by deleting non-relevant characteristics. The objective value of GX is assessed at the conclusion of the exploitation stage, and if it is less than X (t), GX(t_i) replaces X(t) as the best solution (silverback). The accuracy is shown in Fig. 10. The resultant features are finally classified using a two-level classifier.

The parameters for these approaches are the same as those described in Table V.

TABLE V. DIFFERENT METAHEURISTIC ALGORITHM PARAMETERS

Algorithms	Parameters Settings	Values
General Settings	Population Size(N) Max numb of Iterations (M) Considered Strategy	20 50(Max) Features
PSO	Acceleration Coefficients (C_1) (C_2) Inertia Weight (W) Numb of Iterations	[0.5:2.5] [0.5:2.5] [0.2:0.9] 30
GTO	Beta(β) w p	3 0.8 0.03
ACO	Starting Ant Pheromone Pheromone-exponential-wt Ant Pheromone evaporation Numb of Iterations Population Size(number of Ant)	1 1 0.05 30 5

I. Two-Level Classification

For more accurate results, the final characteristics are classified using two-level classification. Given an image I = $\{I_i\}_{i=1}^{N}$, where $I_i \in [0, 255]^3$ corresponds to one of the seven types of lesion types, the deep neural model performs a series of operations to determine the type of an image I ∈ {1...,7}. A function can be used to express these operations as shown in (23).

$$F(I, W_m) = \underset{M}{argmax}\ y_M \quad (23)$$

where W_m is the specifications of the train neural model & y_m are the type probabilities generated by the model.

The presence of unbalanced classes in the dataset is one of the issues that arise during the training stage of any classification model. To assess and handle these scenarios, duo distinct prediction approaches for the deep learning models are proposed:

1) Single level classifier: Transfer learning is used to tune the weights of a neural model. This method assigns the input image to one of the two categories. In this case, the impact of unbalanced classes can be significant, necessitating the use of a preprocessing stage to optimize performance. The single level classifier's operation is as follows in (24):

$$F^P(I, W^P) = argmax\ y_M,\ M \in \{1,2\} \quad (24)$$

where W^P indicates the specifications of the refined network for the two categories of epidermis lesions.

2) Two-level classifier: Two neural models are combined in this technique to create a two-level classifier. While the second level categorizes the other multiple classes, the first level has been trained to differentiate between the malignant melanoma class and the others. as shown in (25,26):

$$F_{c_1}(I, W_{c_1}) = \text{argmax } \{y, y'\} \quad (25)$$

$$F_{c_2}(I, W_{c_2}) = argmax\ y_M,\ M \in \{2...,7\} \quad (26)$$

where the refined model for two and six subclasses, respectively, is represented by W_{c_1}. The initial neuron model is transformed into a specialized model that serves as a classification model for the malignant melanoma class, which includes the binary classification on the dataset's images. Only if $F_{c_1}(I, W_{c_1})$ fails to produce the melanoma class is the second classifier used.

V. Results and Discussions

This section compares the proposed optimization method to other metaheuristic feature selection algorithms in order to assess its effectiveness in identifying the best subset of features, such as the original PSO from Fig. 11, ACO from Fig. 12 and GTO shown from Fig. 13. All of these techniques are used on the HAM10000 dataset.

A. Experiments Configuration

It is described how the experiments were set up for this study in Table VI:

TABLE VI. Configuration Details

Configurations	Specification
Input Image Size	(150x150x3)
MHFS Optimizers	PSO, ACO, GTO
Dataset Split ratio	70-10-20(Tr-V-Ts)
Population Size	30
Epochs Count	50(Max)
Activation Function	Softmax
Pretrained Model	ResNet, Inception, VGG16
Losses Range	Categorical Crossentropy
Parameters optimizer Range	RMSprop, Adam, SGD
Dropout Count	[0:0.6]
Batch Size Range	[4:30]
Technologies	Tensorflow, Keras, Numpy, OpenCV, Matplotlib
Scripting Language	Python
Work Environment	Google Colab with GPU

B. Performance Evaluation

The performance of proposed model was analyzed with the standard classification measures: Accuracy, Precision, Recall (28) and F-measure. It is well known that recall equals the ratio of relevant instances retrieved over the total number of relevant examples, precision equals the proportion of relevant instances among the retrieved instances, and accuracy equals the proportion of genuine detentions from (27, 29). By considering both precision and recall, the F-measure from (30) offers a good overall evaluation of the effectiveness of a particular approach. All metrics are ranked from [0 to 1], with 1 being the best. Below Table VII shows original deep features, Table VIII describes features from PSO, Table IX describes features from ACO, and Table X describes features from GTO extracted from metaheuristic algorithms.

Each metric is formulated as follows:

$$\text{Accuracy} = \frac{TP+TN}{TP+FP+FN+TN} \quad (27)$$

$$\text{Recall (Sensitivity)} = \frac{TP}{TP+FN} \quad (28)$$

$$\text{Precision} = \frac{TP}{TP+FP} \quad (29)$$

$$\text{F-Measure} = 2.\frac{Precision.Recall}{Precision+Recall} \quad (30)$$

This work yielded the following results for the suggested framework:

TABLE VII. Classification Accuracy using Originally Extracted Features for HAM10000

Classifier	Accuracy	Recall	Precision	F-Measure
Single-Level	0.85	0.82	0.86	0.84
Two-Level	0.83	0.81	0.89	0.85

The result analysis using various metaheuristic techniques is depicted below.

TABLE VIII. Classification Accuracy based on PSO Selected Features Approach

Classifier	Accuracy	Recall	Precision	F-Measure
Single-Level	0.85	0.83	0.87	0.8
Two-Level	0.93	0.85	0.89	0.87

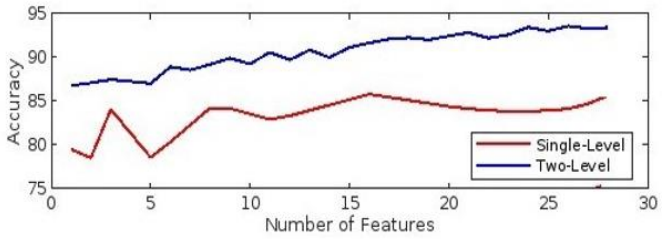

Fig. 11. PSO Selected Features vs. Accuracy.

TABLE IX. Classification Accuracy based on ACO Selected Features Approach

Classifier	Accuracy	Recall	Precision	F-Measure
Single-Level	0.76	0.74	0.80	0.77
Two-Level	0.84	0.80	0.90	0.84

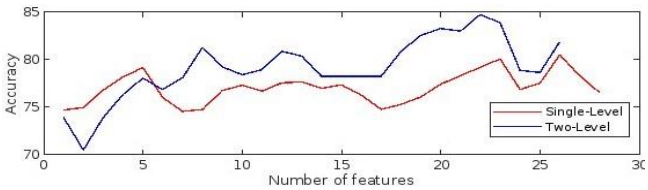

Fig. 12. ACO Selected Features vs. Accuracy.

TABLE X. CLASSIFICATION ACCURACY BASED ON GTO SELECTED FEATURES APPROACH

Classifier	Accuracy	Recall	Precision	F-Measure
Single-Level	0.89	0.84	0.90	0.87
Two-Level	0.93	0.83	0.89	0.86

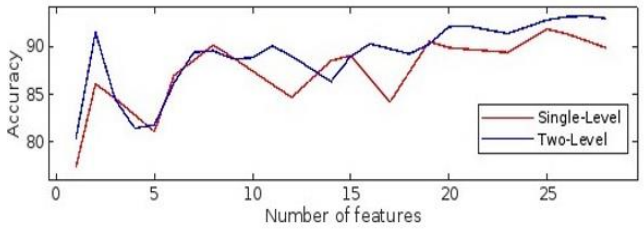

Fig. 13. GTO Selected Features vs. Accuracy.

1) Result comparison: The comparative assessment among various similar works using the HAM10000 dataset is shown in Table XI and Fig. 14. In comparison to other related works, the proposed work performs significantly better in terms of classification accuracy with the fewest features.

TABLE XI. COMPARISON ANALYSIS WITH OTHER STATE-OF-ART METHODS USING HAM10000 DATASET

Paper Id	Methodology	Accuracy %
[38]	PCA	89.8
[39]	Bayesian deep learning	83.59
[40]	Transfer learning	85.0
[41]	CNN	80.0
[42]	Application based CNN	78.0
[43]	MobileNet	83.2
[44]	ResNet50+InceptionV3	89.9
Proposed Work	NasNet Large	93.58

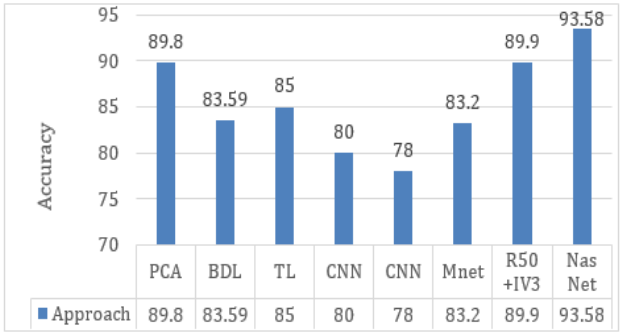

Fig. 14. Comparison of Various Deep Learning Approaches of Accuracy on HAM10000 Dataset.

VI. CONCLUSION

The rising cost of epidermis cancer therapy throws life tough for survivors and their families. Early identification of melanoma skin cancer is critical to curing the condition. In this paper, we proposed two approaches based on domain adaptation for computer-aided diagnosis of skin cancers. We attempted to categorize the other five forms of skin illnesses in addition to the typical non-melanoma and melanoma groups. The NAS strategy and the tools offered were designed to help optimize the model and, as a result, improve research findings. Using the HAM10000 dataset, two alternative recommended models were used: a single level and a two level, the first of which clears in distinguishing between melanoma and non-melanoma images and the second with classifying benign lesions. In this study, the GTO algorithm for selecting features outperforms the PSO and ACO feature selection algorithms. The goal of this study was to provide a feature selection (FS) strategy by increasing the performance of the Gorilla Troops Optimizer (GTO). GTO feature selection algorithm selects set of optimized feature to provide deliver classification accuracy of 89.89 and 93.58. The limitation of the proposed model was computational time. Though the NasNet itself takes time to generate the desired model, feature optimization is additionally added. The aim was met due to finite computational resources within a reasonable period which is a desirable in the field of medical imaging. It is not possible to declare that the most ideal architecture was discovered, but the best-known architecture was attained.

Funding Statement: The authors received no specific funding for this study.

Conflict of Interest: The authors declare that they have no conflicts of interest.

Availability of data and material (data transparency): The data are publicly available at https://challenge.isic-archive.com/data/

REFERENCES

[1] Leiter, U.; Eigentler, T.; Garbe, C. “Epidemiology of skin cancer. In Sunlight, Vitamin D and Skin Cance”r; Springer: Berlin/Heidelberg, Germany, pp. 120–140,2014.

[2] Dong, Y.; Wang, L.; Cheng, S.; Li, Y. “FAC-Net: Feedback Attention Network Based on Context Encoder Network for Skin Lesion Segmentation”. Sensors 21, 5172,2021.

[3] Dildar M, Akram S, Irfan M, Khan HU, Ramzan M, Mahmood AR, Alsaiari SA, Saeed AH, Alraddadi MO, Mahnashi MH. Skin cancer detection: a review using deep learning techniques. International journal of environmental research and public health. 2021 Jan;18(10):5479.

[4] Akram, T.; Sharif, M.; Saba, T.; Javed, K.; Lali, I.U.; Tanik, U.J.; Rehman, A. Construction of saliency map and hybrid set of features for efficient segmentation and classification of skin lesion. Microsc. Res. Tech. 82, 741–763,2019.

[5] Singer S, Tkachenko E, Hartman RI, Mostaghimi A. Gender identity and lifetime prevalence of skin cancer in the United States. JAMA dermatology Apr 1;156(4):458-60, 2020.

[6] Alom MZ, Aspiras T, Taha TM, Asari VK. Skin cancer segmentation and classification with NABLA-N and inception recurrent residual convolutional networks. arXiv preprint arXiv:1904.11126. 2019 Apr 25.

[7] Ge Z, Demyanov S, Chakravorty R, Bowling A, Garnavi R. Skin disease recognition using deep saliency features and multimodal learning of dermoscopy and clinical images. InInternational Conference on Medical Image Computing and Computer-Assisted Intervention Sep 10 (pp. 250-258). Springer, Cham,2017.

[8] Gouabou, A.F.; Damoiseaux, J.-L.; Monnier, J.; Iguernaissi, R.; Moudafi, A.; Merad, D. Ensemble Method of Convolutional Neural Networks with Directed Acyclic Graph Using Dermoscopic Images: Melanoma Detection Application. Sensors 21, 3999,2021.

[9] Bafounta, M.-L.; Beauchet, A.; Aegerter, P.; Saiag, P. Is dermoscopy (epiluminescence microscopy) useful for the diagnosis of melanoma: Results of a meta-analysis using techniques adapted to the evaluation of diagnostic tests. Arch. Dermatol 137, 1343–1350,2001.

[10] Argenziano, G.; Soyer, H.P.; Chimenti, S.; Talamini, R.; Corona, R.; Sera, F.; Binder, M.; Cerroni, L.; De Rosa, G.; Ferrara, G.; et al. Dermoscopy of pigmented skin lesions: Results of a consensus meeting via the Internet. J. Am. Acad. Dermatol 48, 679–693,2003.

[11] Sharif, M.; Akram, T.; Kadry, S.; Hsu, C.-H. A two-stream deep neural network-based intelligent system for complex skin cancer types classification. Int. J. Intell. Syst. 2021.

[12] Alhaisoni, M.; Tariq, U.; Hussain, N.; Majid, A.; Damaševi˘cius, R.; Maskeliunas, R. COVID-19 Case Recognition from Chest CT ¯ Images by Deep Learning, Entropy-Controlled Firefly Optimization, and Parallel Feature Fusion. Sensors 21, 7286, 2021.

[13] Khan, M.A.; Muhammad, K.; Sharif, M.; Akram, T.; Kadry, S. Intelligent fusion-assisted skin lesion localization and classification for smart healthcare. Neural Comput. Appl 1–16, 2021.

[14] Dey, S.; Roychoudhury, R.; Malakar, S.; Sarkar, R. An optimized fuzzy ensemble of convolutional neural networks for detecting tuberculosis from Chest X-ray images. Appl. Soft Comput. 114, 108094, 2021.

[15] Khamparia, A.; Singh, P.K.; Rani, P.; Samanta, D.; Khanna, A.; Bhushan, B. An internet of health things-driven deep learning framework for detection and classification of skin cancer using transfer learning. Trans. Emerg. Telecommun. Technol. 32, e3963, 2020.

[16] Akram, T.; Sharif, M.; Shahzad, A.; Aurangzeb, K.; Alhussein, M.; Haider, S.I.; Altamrah, A. An implementation of normal distribution-based segmentation and entropy-controlled features selection for skin lesion detection and classification. BMC Cancer 18, 638, 2018.

[17] Codella, Noel CF, et al. "Skin lesion analysis toward melanoma detection: A challenge at the 2017 international symposium on biomedical imaging (isbi), hosted by the international skin imaging collaboration (isic)." 2018 IEEE 15th international symposium on biomedical imaging (ISBI 2018). IEEE, 2018.

[18] Zafar, K.; Gilani, S.O.; Waris, A.; Ahmed, A.; Jamil, M.; Khan, M.N.; Sohail Kashif, A. Skin Lesion Segmentation from Dermoscopic Images Using Convolutional Neural Network. Sensors 2020, 20, 1601.

[19] Song, L.; Lin, J.P.; Wang, Z.J.; Wang, H. An End-to-End Multi-Task Deep Learning Framework for Skin Lesion Analysis. IEEE J. Biomed. Health Inform. 24, 2912–2921, 2020.

[20] Aziz, S.; Bilal, M.; Khan, M.U.; Amjad, F. Deep Learning-based Automatic Morphological Classification of Leukocytes Using Blood Smears. In Proceedings of the 2020 International Conference on Electrical, Communication, and Computer Engineering (ICECCE), Istanbul, Turkey, 14–15 April pp. 1–5, 2020.

[21] Ren, Y.; Yu, L.; Tian, S.; Cheng, J.; Guo, Z.; Zhang, Y. Serial attention network for skin lesion segmentation. J. Ambient. Intell. Humaniz. Comput. 1–12, 2021.

[22] Xie, Y.; Zhang, J.; Xia, Y.; Shen, C. A Mutual Bootstrapping Model for Automated Skin Lesion Segmentation and Classification. IEEE Trans. Med. Imaging 39, 2482–2493,2020.

[23] Zhang, J.; Xie, Y.; Xia, Y.; Shen, C. Attention residual learning for skin lesion classification. IEEE Trans. Med. Imaging 38, 2092–2103, 2019.

[24] Yu L, Chen H, Dou Q, Qin J, Heng P-A. Automated melanoma recognition in dermoscopy images via very deep residual networks. IEEE Trans Med Imaging 36(4):994–1004, 2016.

[25] Majtner T, Yildirim-Yayilgan S, Hardeberg JY. Combining deep learning and hand-crafted features for skin lesion classification. In: 2016 Sixth international conference on image processing theory, tools and applications. IEEE, p. 1–6, 2016.

[26] Ahonen T, Hadid A, Pietikainen M. Face description with local binary patterns: Application to face recognition. IEEE Trans Pattern Anal Mach Intell 28(12):2037–41, 2006.

[27] Arivuselvam B. Skin Cancer Detection and Classification Using Svm Classifier. Turkish Journal of Computer and Mathematics Education (TURCOMAT). 2021 Jun 4;12(13):1863-71.

[28] T. Elsken, J. H. Metzen, and F. Hutter, ''Neural architecture search: A survey,'' J. Mach. Learn. Res., vol. 20, pp. 55:1-55:21, Mar. 2019.

[29] B. Zoph, V. Vasudevan, J. Shlens, and Q. V. Le, ''Learning transferable architectures for scalable image recognition,'' in Proc. IEEE/CVF Conf. Comput. Vis. Pattern Recognit., Salt Lake City, UT, USA, Jun pp. 8697–8710, 2018.

[30] Termritthikun C, Jamtsho Y, Ieamsaard J, Muneesawang P, Lee I. EEEA-Net: An Early Exit Evolutionary Neural Architecture Search. Engineering Applications of Artificial Intelligence. Sep 1; 104:104397, 2021.

[31] Yu, Z.; Jiang, X.; Zhou, F.; Qin, J.; Ni, D.; Chen, S.; Lei, B.; Wang, T. Melanoma Recognition in Dermoscopy Images via Aggregated Deep Convolutional Features. IEEE Trans. Biomed. Eng. 66, 1006–1016, 2018.

[32] Srinivasu, P.N.; SivaSai, J.G.; Ijaz, M.F.; Bhoi, A.K.; Kim, W.; Kang, J.J. Classification of skin disease using deep learning neural networks with MobileNet V2 and LSTM. Sensors 21, 2852, 2021.

[33] Khan MA, Akram T, Sharif M, Kadry S, Nam Y. Computer decision support system for skin cancer localization and classification (2021).

[34] E.H. Houssein, M.R. Saad, F.A. Hashim, H. Shaban, M. Hassaballah, Lévy Flight distribution: A new metaheuristic algorithm for solving engineering optimization problems, Eng. Appl. Artif. Intell. 94 (2020) 103731.

[35] I.BoussaïD, J. Lepagnot, P. Siarry, A survey on optimization metaheuristics, Inform. Sci. 237 82–117, (2013).

[36] Hashim FA, Houssein EH, Hussain K, Mabrouk MS, Al-Atabany W. Honey Badger Algorithm: New metaheuristic algorithm for solving optimization problems. Mathematics and Computers in Simulation. Feb 1; 192:84-110, 2022.

[37] F. Hashim, M.S. Mabrouk, W. Al-Atabany, Gwomf: Grey wolf optimization for motif finding, in 2017 13th International Computer Engineering Conference (ICENCO), IEEE, pp. 141–146, 2017.

[38] Khan MA, Javed MY, Sharif M, Saba T, Rehman A (2019) Multi-model deep neural network based features extraction and optimal selection approach for skin lesion classification. In: 2019 international conference on computer and information sciences (ICCIS). IEEE, pp 1–7.

[39] Mobiny A, Singh A, Van Nguyen H Risk-aware machine learning classifier for skin lesion diagnosis. J Clin Med 8(8):1241, (2019).

[40] Moldovan D Transfer learning based method for two-step skin cancer images classification. In: 2019 E-health and bioengineering conference (EHB), pp 1–4, (2019).

[41] Nugroho AA, Slamet I, Sugiyanto Skins cancer identification system of HAMl0000 skin cancer dataset using convolutional neural network. AIP Conf Proc 2202(1):020039, (2019).

[42] Pai K, Giridharan A Convolutional neural networks for classifying skin lesions. In: TENCON 2019—2019 IEEE region 10 conference (TENCON). IEEE, pp 1794–1796, (2019).

[43] Sae-Lim W, Wettayaprasit W, Aiyarak P (2019) Convolutional neural networks using MobileNet for skin lesion classification. In: 16th international joint conference on computer science and software engineering (JCSSE), pp 242–247, 2019.

[44] Shahin AH, Kamal A, Elattar MA Deep ensemble learning for skin lesion classification from dermoscopic images. In: 2018 9th Cairo international biomedical engineering conference (CIBEC). IEEE, pp 150–153, (2018).

[45] Tsang, S. H.Review: Nasnet-neural architecture search network (image classification), 2020.

[46] Fong, S., Wong, R., & Vasilakos, A. V. Accelerated PSO Swarm Search Feature Selection for Data Stream Mining Big Data. IEEE Transactions on Services Computing, 9(1), 33–45. doi:10.1109/TSC.2015.2439695, (2016).

[47] Seijas, L.M. Metaheuristics for feature selection in handwritten digit recognition. 2015 Latin America Congress on Computational Intelligence (LA-CCI), 1-6. doi: 10.1109/LA-CCI.2015.7435975, (2015).

[48] Yeh, J., & Chan, S. Population-based metaheuristic approaches for feature selection on mammograms. 2017 IEEE International Conference on Agents (ICA), 140-144. doi:10.1109/AGENTS.2017.8015321, (2017).

[49] Naeini, A. A., Babadi, M., Mirzadeh, S. M. J., & Amini, S. Particle Swarm Optimization for Object-Based Feature Selection of VHSR Satellite Images. IEEE Geoscience and Remote Sensing Letters, 15(3), 379–383. doi:10.1109/LGRS.2017.2789194, (2018).

[50] Ighazran, H., Alaoui, L., & Boujiha, T. Metaheuristic and Evolutionary Methods for Feature Selection in Sentiment Analysis (a Comparative Study). International Symposium on Advanced Electrical and Communication Technologies(ISAECT),1-6, doi:10.1109/ISAECT.2018.8618799, (2018).

[51] Arora, S., Singh, H., Sharma, M., Sharma, S., & Anand, P. A New Hybrid Algorithm based on Grey Wolf Optimization and Crow Search Algorithm for unconstrained function optimization and feature selection. IEEE. doi:10.1109/ACCESS.2019.2897325, (2019).

[52] Kondaveeti HK, Edupuganti P. Skin cancer classification using transfer learning. In2020 IEEE International Conference on Advent Trends in Multidisciplinary Research and Innovation (ICATMRI) 2020 Dec 30 (pp. 1-4). IEEE.

[53] B. Zoph, V. Vasudevan, J. Shlens and Q. V. Le, "Learning Transferable Architectures for Scalable Image Recognition," 2018 IEEE/CVF Conference on Computer Vision and Pattern Recognition, pp. 8697-8710, doi: 10.1109/CVPR.2018.00907, 2018.

[54] Shi X, Dou Q, Xue C, Qin J, Chen H, Heng PA. An active learning approach for reducing annotation cost in skin lesion analysis. InInternational Workshop on Machine Learning in Medical Imaging Oct 13 (pp. 628-636). Springer, Cham, 2019.

[55] Mukherjee S, Adhikari A, Roy M. Melanoma Detection from Lesion Images Using Optimized Features Selected by Metaheuristic Algorithms. International Journal of Healthcare Information Systems and Informatics (IJHISI). 2021 Oct 1;16(4):1-22.

[56] Aurora, S., Begoña, A., & Carmen, S. Pattern Analysis in Dermoscopic Images. In J. Scharcanski (Ed.), Computer Vision Techniques for the Diagnosis of Skin Cancer. Series in Bioengineering. doi:10.1007/978-3-642-39608-3_2, (2014).

[57] Mukherjee S, Adhikari A, Roy M. Malignant melanoma detection using multi-layer perceptron with optimized network parameter selection by pso. InContemporary advances in innovative and applicable information technology 2019 (pp. 101-109). Springer,Singapore.